Sudden eutrophication of an aluminum sulphate treated lake due to abrupt increase of internal phosphorus loading after three decades of mesotrophy

Tallent Dadi*[1], Martin Schultze[1], Xiangzhen Kong[1,2], Michael Seewald[1], Karsten Rinke[1], Kurt Friese[1]

[1]UFZ-Helmholtz Centre for Environmental Research, Department Lake Research, Brueckstr. 3a, D-39114 Magdeburg, Germany

[2]State Key Laboratory of Lake Science and Environment, Nanjing Institute of Geography and Limnology, Chinese Academy of Sciences, 210008 Nanjing, China

*****Correspondence: tallent.dadi@ufz.de

Abstract

Aluminum salts are widely used to immobilize phosphorus (P) in lakes suffering from internal loading. However, longevity of treatments varies among lakes; some lakes eutrophy faster than others. We conducted biogeochemical investigations of sediments of closed artificial Lake Barleber, Germany that was successfully remediated with aluminum sulphate in 1986. The lake became mesotrophic for almost 30 years; a rather rapid re-eutrophication took place in 2016 leading to massive cyanobacterial blooms. We quantified internal loading from sediment and analyzed two environmental factors that might have contributed to the sudden shift in trophic state. Increase in lake P concentration started in 2016, reaching 0.3 mg L^{-1}, and remained elevated into the spring of 2018. Reducible P fraction in the sediment was 37 - 58% of total P, indicating a high potential for mobilization of benthic P during anoxia. Estimated P release from sediments for 2017 was approximately 600 kg for the whole lake. This is consistent with sediment incubation results; higher temperature (20°C) and anoxia contributed to release of P (27.9 ± 7.1 mg m^{-2} d^{-1}, 0.94 ± 0.23 mmol m^{-2} d^{-1}) to the lake, triggering re-eutrophication. Loss of aluminum P adsorption capacity together with anoxia and high water temperatures (organic matter mineralization) are major drivers of re-eutrophication. Accordingly, treated lakes at some time require a repeated aluminum treatment for sustaining acceptable water quality and we recommend regular sediment monitoring in treated lakes. This is crucial given the effects of climate warming on duration of stratification in lakes which may result in the need for treatment of many lakes.

Keywords

Internal phosphorus loading, aluminum sulphate, redox conditions, sediment P-fractionation, lake restoration success

1. Introduction

Internal loading of excessive nutrient is often a long-lasting problem in lakes that suffered from long-lasting external nutrient loading (Foy 1985, Jeppesen et al. 2005). These lakes could remain eutrophic over a decade even after external loads have been reduced due to high P-release from sediments (Søndergaard et al. 2005). Application of P-binding agents in lake restoration has been practiced by lake managers for several decades (Huser et al. 2016, Lürling and Oosterhout 2013). Among the early treatments, water column P was low and stable for just a few years after treatment, whereas in other cases, long-term stabilisation of low-P concentrations in the water column lasted more than 30 years (Huser et al. 2016).

Although it is known that lakes treated to immobilize P can switch back to a eutrophic state after decades of high water quality, studies are rare that quantify responsible mechanisms because restoration efforts are not paralleled by concurrent water quality monitoring over the scale of decades, and sediment studies are also only rarely done in such lakes. Here, we provide P dynamics in a lake that switched its trophic state back towards eutrophy – a phenomenon we call ‘re-eutrophication’.

Re-eutrophication is likely to occur in shallow lakes i.e. <3 - 10 m (Mesman et al. 2021) because of their higher ratio of sediment surface to water volume and higher temperature. There are several potential reasons for re-eutrophication: insufficient reduction of external P loading (Huser et al. 2016), changes in the catchment leading to increased external P loading (Jarvie et al. 2017); saturation of the addition to P adsorption capacity from added P-binding agents (Berkowitz et al. 2006); excessive historical P in the sediment mobilized through sediment resuspension by wind or benthivorous fish (Jeppesen et al. 2005); and high concentration of P bound to redox-dependent iron hydroxides, which is mobilized during anoxia (Einsele 1936, Mortimer 1942). However, for lakes with intermediate depth, the cause of re-eutrophication may be complex and far from conclusive because, although also quite shallow, they can become stratified and anoxic (Mesman et al. 2021).

Lakes of shallow to intermediate depth are prone to shorter-term stratification, i.e. polymictic with sporadic anoxia in the deeper water, which may result in release of redox sensitive P and subsequent decrease in N:P ratios (Shatwell and Köhler 2019). This can trigger self-enhancing eutrophication. In contrast to deep stratified lakes (where summer anoxia commonly only results in temporary accumulation of P in the hypolimnion, particularly in its deepest layers), anoxia in a lake of intermediate depth can result in rapid transport of released P into the euphotic zone by subsequent mixing events (Taranu et al. 2012). Therefore, mixing events are a shortcut between sediments and the photic zone, suppling P to the photic zone. Transfer of P from sediment to the euphotic zone can occur in hours.

Transfer of P from the hypolimnion to the epilimnion is typically wind-induced, accompanying deepening of the epilimnion, and erosion of the upper hypolimnion.

This paper focuses on Lake Barleber, a closed lake formed by gravel mining in central Germany; restoration was successful for nearly 30 years; a rather rapid increase in P concentration led to excessive cyanobacteria bloom in summer 2017, which prompted investigations into potential cause(s) of the re-eutrophication (Rinke et al. 2018; Kong et al. 2021; Rönicke et al. 2021). We seek to understand and highlight reasons for re-occurrence of P release from lake sediments after Al-treatment and to determine and quantify underlying processes. We hypothesize that nutrient enrichment was due to internal lake processes because the lake has no surface water inflows and almost all sediment is autochthonous. Gravel excavation lakes, like Lake Barleber, are widely distributed in the world and provide valuable habitats and ecosystem services (Mollema and Antonellini 2016, Seelen et al. 2022); therefore, management issues for Lake Barleber may apply to many of these artificial lakes with intermediate depth and low external loading.

First, we wanted to quantify if increased internal loading explains the sudden re-eutrophication of Lake Barleber. Second, if this is true, which combination of environmental factors contributed to the sudden shift in trophic state after almost three decades of low trophy invoked by an aluminum treatment in 1986? We investigated the causes of the re-eutrophication in Lake Barleber by quantifying release of redox-dependent P during phases of anoxia by multiple approaches. We employed sediment incubation at different temperature and oxygen conditions, P fractionation in the sediment, and general sediment characterization to determine main processes of P release and quantify the solute inventory in the sediment. We then compared these results with observed P dynamics in the field. Because internal P loading in Lake Barleber was substantially reduced by aluminium in autumn 1986 (Rönicke et al. 2021), our findings are important for understanding the long-term processes regulating P in such lakes and for evaluating the effective duration of lake restoration techniques using aluminium salts.

2. Materials and Methods

2.1 Site description and historical monitoring data

Lake Barleber is an artificial lake located near Magdeburg, Germany (52° 13‘15‘‘N, 11° 39‘0‘‘E) (Fig. 1). It has a maximum depth of 11 meters, mean depth of 6.7 meters, area of 103 hectares, and volume of 6.9 million cubic meters (Rönicke et al. 2021). The lake was created from gravel excavation at the beginning of the 1930s (Bauch 1953); it has no surface inflow or outflow but is fed by groundwater. The lake was phytoplankton-dominated during the 1970s of the last century (Klapper and Geller 2001). The eutrophic state threatened the

recreational use of the lake, mostly swimming. To safeguard a sustained recreational use, the lake was successfully remediated in 1986 by applying 480 tonnes of aluminum sulfate (Klapper and Geller 2001). This equates to a total of Al^{3+} dosage of 37 tonnes, a volumetric dosage of 5.7 mg L^{-1} and an areal dosage 36 g m^{-2}. One year later, the lake switched back to a clear water status and macrophytes re-established (Klapper and Geller 2001). In 2017, 31 years after remediation, massive cyanobacterial blooms suddenly re-occurred in the lake. Nutrients concentrations for 2013/2014, 2016 and 2017 are shown in Table 1.

Lake Barleber is monomictic; it experiences thermal stratification. The hypolimnion is very small and restricted to the deepest part of the lake during summer and early autumn (Kong et al. 2021). Stable ice cover and, thus, stable inverse stratification rarely forms.

Lake Barleber has a net groundwater inflow due to the deficit created by evaporation from the lake surface, which is greater than precipitation on the lake. This deficit amounts to 190 mm per year, which translates to an annual volume of 200,000 m^3 (Hannappel and Strom 2020, Rinke et al. 2018). Annual groundwater inflow and outflow are 640,000 and 530,000 m^3 respectively, based on measurements in 2018 and 2019 (Hannappel and Strom 2020). External P loads are low: atmospheric deposition (42 kg yr^{-1}), groundwater (13 kg yr^{-1}) and bathing (10 kg yr^{-1}) contribute insignificantly to the lake's phosphorus dynamics (Hannappel and Strom 2020, Rinke et al. 2018).

To understand the trophic state prior to the massive bloom in 2017, we analyzed Lake Barleber historical surface (integrated epilimnion samples) and hypolimnion water monitoring data; SRP, TP, TN, NH_4^+-N, O_2, chlorophyll *a* and temperature (Flood Protection and Water Management Authority for Saxony Anhalt website (LHW):

(https://lhw.sachsen-anhalt.de/untersuchen-bewerten/monitoringergebnisse/ accessed 11.08.2020).

2.2 Sediment and water sampling

Undisturbed sediment cores were sampled on the 15th of August 2017 and 20th of November 2017 for the sampling points BA1 and BA2 and on the 8th of January 2018 for BA3 (see Fig 1) using a modified Kajak gravity corer (UWITEC, Austria) and plexi-glass tubes (60 cm length and 9 cm inner diameter). Three sediments cores per sampling point for each sampling were extracted for general sediment characterization, porewater analysis and P-fractionation.

In addition, in January 2018, 12 undisturbed sediment cores of approx. 30 cm length and overlying water were retrieved from sampling point BA3 (see Fig 1) for incubation (see below section 2.6). Sampling took place in winter to assure that the sediment-water-interface is oxic (Fig. 2) and sediment pools of P represent the initial conditions before the vegetation period

and potential stratification has started. Cores were closed on top with a special lid which allowed continuous stirring of overlying water. Detailed description of the special lid for sediment cores is given in Dadi et al. (2015).

Water samples were taken directly above the sediment (< 50 cm from sediment) using a standard two litres water sampler (LIMNOS, Turku, Finland) and analyzed for various parameters (see below).

2.3 Water analytics

We analyzed: total phosphorus (TP), total dissolved phosphorus (DP), soluble reactive phosphorus (SRP), dissolved organic carbon (DOC), nitrate (NO_3^--N), ammonium (NH_4^+-N), sulfate (SO_4^{2-}), total dissolved iron (Fe), and total dissolved manganese (Mn). Syringe filters (Sartorius, Germany) of 0.2 µm pore size were used for all needed filtrations. SRP, NO_3^--N, NH_4^+-N, TP and DP (after digestion by persulphate ($K_2S_2O_8$) and sulphuric acid (H_2SO_4) at 100°C for 45 minutes) were analyzed photometrically (Skalar, The Netherlands), DOC was measured with C-analyzer (Dimatoc, Germany), Fe and Mn were determined by ICP-OES (Perkin Elmer, Germany), and SO_4^{2-} was analyzed by ion-chromatography (Dionex) (Friese et al. 2014).

2.4 Sediment characterization

Sediment cores for porewater extraction and P fractionation were sectioned into: 0 - 1, 1 - 2, 2 - 3, 3 - 4, 4 - 5, 5 - 6, 6 - 8, 8 - 10 cm layers. Porewater was extracted by centrifugation (3500 rpm at 8^{o}C) and filtration using 0.45 µm syringe filter (Sartorius, Germany). Porewater samples were analyzed for SRP, dissolved Fe, SO_4^{2-}, NH_4^+-N, and DOC as described in the previous section. Additionally, we sectioned a longer (40 cm) sediment core extracted from the deepest point (BA1) in September 2018.

A volume of 5 mL of homogenized sediment was measured by filling the sediment in an open syringe (cut off the entire tip diameter uniformly) ensuring that there are no air bubbles. The sediment was added to pre-weighed crucibles. Percent water was determined gravimetrically by drying sediment samples at 105^{o}C; loss on ignition (LOI_{550}) was determined by combustion of dry sediment samples at 550^{o}C for 2 hours, for the longer sediment core from BA1 (extracted in 2018) we also carried out LOI_{950} by further combustion of the LOI_{550} samples for 2 hours at 950^{o}C. Total carbon (TC); total organic carbon (TOC, after removal of inorganic carbon by acidification); and total nitrogen (TN) were determined by a CN analyzer vario EL cube (Elementar Analysensysteme GmbH, Hanau). Iron, Al, Mn, and S in sediments were determined by wavelength dispersive X-ray fluorescence (XRF; S4 Pioneer Bruker-AXS) following Morgenstern et al. (2001). Dry density for each sediment layer was calculated by dividing the sediment dry weight by the volume of wet sediment.

2.5 Sediment P-fractionation

Phosphorus fractionation was carried out using the method of Psenner et al. (1984), modified by Hupfer et al. (1995). Phosphorus fractionation was developed to distinguish among the concentrations of various metals (Fe, Mn, and Al), $CaCO_3$, and organically bound P fractions by using various extracting solutions. The five successive P fractions obtained are:

i. 1M NH_4Cl (NH_4Cl-P): easily available P in porewater (NRP – non-reactive P and SRP);
ii. 0.11M $NaHCO_3$/ 0.11M $Na_2S_2O_4$ (BD-P): redox-dependent (Fe bound) P ;
iii. 1M NaOH (NaOH-P): Al bound P , the fraction is subdivided into NaOH-SRP (OH^- exchangeable P) and NaOH-NRP (organic bound P and NRP);
iv. 0.5M HCl (HCl-P): P bound by carbonates and apatite;
v. Residual-P: refractory P determined after digestion of remaining sediment with ($K_2S_2O_8$) and H_2SO_4 at 100°C for 45 minutes.

Sum of the P fractions is used as TP. The Ca, Al, Fe and Mn concentration in the fractions of the sediment core from BA1, September 2018 were also determined.

Various molar ratios were calculated to assess the P retention capacity. A (NH4Cl + BD + NaOH)-Al : (NH4Cl + BD + NaOH)-Fe ratio >3 and a NaOH-Al : (NH4Cl + BD)-P ratio > 25, have been shown to prevent P release from lake sediments (Kopáček et al. 2005). A NaOH-Al : NaOH-P molar ratio of >12.6 has been proposed by (Rydin and Welch 2000) as ideal for P retention; the ratio is higher just after treatment and decreases over time (Huser 2017). NaOH-Al : BD-Fe ratios represent the major fractions involved in P retention; a threshold value >11 being ideal to prevent P-release (Nürnberg et al. 2018).

2.6 Sediment incubation

2.6.1 Experimental design

Sediment cores were incubated for 35 days in climate chambers at 6°C and 20°C, and oxic/anoxic conditions in the overlying water. Lower temperature was the *in-situ* lake temperature at the time of sampling (ca. 4^{o}C and similar to the hypolimnetic temperatures during early spring. Higher temperature was chosen as a realistic maximum sediment temperature for epilimnetic sediments in summer. Epilimnetic sediments in Lake Barleber extend to 8 m depth and therefore comprise more than 90% of the total sediment area. Experimental setup thus was a crossed 2 x 2-factorial approach with 3 replicates cores, with temperature and oxic state as factors, each with two values, resulting in four treatment combinations: oxic 6°C, oxic 20°C, anoxic 6°C, and anoxic, 20°C.

Cores were wrapped with aluminum foil to avoid light penetration and algal growth. Cores were oxic prior to sampling, anoxia was achieved by bubbling the overlying water phase of the cores with a mixture of N_2 and CO_2 (99.96 % N_2/0.04 % CO_2). To maintain oxic conditions in the oxic treatments, overlying water of cores was gently bubbled with air using aquarium pumps without inducing resuspension of sediment material. Dissolved oxygen was monitored by optical O_2 sensors (Pyro Science, Germany). Oxygen consumption rate was calculated as the rate of change in O_2 concentration over time multiplied by the volume of overlying water and divided by surface area of the sediment core (equation 1, section 2.6.2).

Redox potential, pH, and temperature were measured in the overlying water during sampling with a multi-parameter meter fitted with conventional pH and redox potential electrodes (WTW Multi3430, Germany). To convert measured oxidation-reduction potential (ORP) to the standard hydrogen electrode potential, a correction of +221 mV at 5°C and +211 mV at 20°C was applied. We sampled 140 mL water for chemical analyses from the sediment cores and we refilled the cores with 140 mL of water from the lake; the refill water was sampled in the lake about 50 cm from the sediment at the time when we extracted the sediments from the lake. Refill water was stored at the same temperature and oxygen status as the treatment, i.e. anoxic treatment received water that had been treated by bubbling with a mixture of nitrogen and carbon dioxide in order to remove the initially present oxygen. As a control for each treatment, 0.5 L replacement water was introduced into a glass bottle and incubated at the same conditions as the cores. This was done to separate the changes due to sediment from the changes occurring in free water and independent of the sediment-water interaction. The water overlying the sediment-water interface in each core was sampled 9 times during the 35-day incubation period (on days 2, 3, 4, 7, 10, 14, 17, 21, 35). Controls were sampled every second sampling of the sediment cores. All samples were analyzed as described in section 2.3 above.

2.6.2 Calculation of solute release rates

Calculation of solute-flux for the incubation experiment was performed using the equation below from (Steinman et al. 2004):

$$Solute_{flux} = (C_t - C_0) \cdot V \cdot A^{-1} \cdot t^{-1} \quad [1]$$

With, $Solute_{flux}$ = Solute-release rate in [mg m^{-2} d^{-1}], C_t = Solute-concentration at time t in [mg L^{-1}], C_0 = Solute-concentration at t=0 in [mg L^{-1}], V = Volume of water column in liters [L], A = sediment surface area in [m^2], t = experiment duration in days [d]

Equation (1) describes a linear relationship of the solute-flux over time. All experiments were done in triplicate therefore the slope of the regression line from the linear fit was used instead

241 of the term $(C_t - C_0)$. Positive values indicate phosphorus release from the sediment,
242 negative values adsorption or binding of P to the sediment.

243 **2.7 Water and sediment P budgets**

244 We quantified P in the lake in summer based on vertical gradients of TP concentration along
245 the vertical axis of Lake Barleber in summer 2017 (algal bloom) and in previous summers (no
246 algal blooms). We quantified total mass of phosphorus in open water of Lake Barleber from
247 vertical profiles of TP, at least sampled at four different depths (maximum was seven depths)
248 and calculated a volume-weighted total TP content by using bathymetric data of Lake
249 Barleber.

250 We estimated annual total amount of P released in 2017 from the P flux rates and lake
251 surface area. These estimates were compared to the quantity of P in water and in the
252 sediment.

253 **2.8 Osgood Index**

254 The Osgood index (Osgood 1988) was calculated to estimate the mixing intensity of the lake
255 and to assess effects of lake morphology on treatment longevity (Huser et al. 2016):

256 $$Osgood\ Index = Z_m/(A)^{0.5} \quad [3]$$

257 where Z_m is mean water column depth [m] and A is lake surface area [km^2]. When Osgood
258 index is above seven it indicates that the lake has stable summer stratification and a lower
259 resuspension potential. Lakes with an Osgood index below seven have unstable
260 stratification, are potentially polymictic, and have a higher sediment resuspension potential.

261 **2.8 Statistics**

262 We used t-tests to determine if the incubation fluxes from manipulations were significantly
263 different from zero. We used ANOVA to test whether fluxes of the four treatments were
264 significantly different from each other. Tukey HSD-test was used for post-hoc comparisons.
265 All statistics were done using SPSS version 22.

266

3. Results

3.1 Physical structure and water quality

At the time of sampling in August 2017, the lake was stratified below 6 m; with anoxia in the hypolimnion; in November 2017 and January 2018, the lake was mixed (Fig. 2). The hypolimnion created when the lake stratifies is very small (Kong et al. 2021). The lake has an Osgood index of 6.6. The pH varied with season (Fig. 2); high pH of up to 10 occurred during the peak of algal blooms.

Historical monitoring data for 2010, 2013, and 2014 were very similar and characterized by relatively low concentrations of N and P (Fig. 3). In all years, the oxygen concentration dropped to values below 2 mg L^{-1} in summer. The seasonal temperature trend close to the sediment was also very similar in all years. Increases for nutrients began during the growing season of 2016; elevated nutrient concentrations persisted over winter into 2017 (Fig. 3). In 2016, the SRP and NH_4-N hypolimnion concentrations were 1 and 2 mg L^{-1}, respectively; in 2017 these concentrations doubled (Fig. 3)

3.2 Porewater and sediment characteristics

The solute gradients between porewater and bottom water favored release of nutrients into overlying water, i.e., concentrations of solutes were higher in porewater than in overlying water (Fig. 4) in particular for DOC, Fe, Mn, and NH_4^+-N. Seasonal and spatial variability was high for SRP, DOC, SO_4^{2-}, Mn, and NH_4^+-N (Fig. 4).

Oxidation-reduction potential (ORP) ranged between -157 and 20 mV; it decreased in the upper 3 cm and remained constant in the lower sediment (Fig. 5). Percent water decreased with depth (Fig. 5) with a considerable difference between the surface sediment (>90%) and the bottom of the core (>60%). Sediment pH ranged from 7.5 to 8.1 across the sampling points but was constant with depth. TP, LOI, TC, and TN were generally higher in the upper sediment than lower sediment; there was a positive correlation of TP and TC (Pearson r = 0.93, n=5) and TP and TN (Pearson r = 0.98, n=5). Aluminum, Fe, and S concentrations were rather constant (Fig. 5).

3.2.1 P-fractionation

Total phosphorus and the respective fractions in upper layers were systematically higher than in bottom layers (Fig. 6) and showed strongest gradients generally in the upper 2 cm. The TP at point BA1 in August 2017 was distinctly higher than for other sampling points in the upper 4 cm (Fig. 6). The mean TP concentration in the upper 5 cm sediment was 1 mg P g^{-1} solid sediment in four cores; an exception was the sediment core taken in August 2017 which had a high TP concentration of 5 mg P g^{-1} (Fig. 6). The upper 3 cm of sediment were

dominated by redox sensitive BD-P, which constituted 37 - 58% of total P in the sediment (Fig. 6) while the remaining part was mainly organic bound NaOH-NRP (25-39%) and carbonate and apatite bound HCl-P (15 - 32%). The sediment below 3 cm had a balanced proportion of the BD and NaOH and HCl fractions. Based on BD-P fraction in the surface layers, the sediments can be characterised as highly sensitive to P-release through anoxia and reductive redox conditions, which agrees with the incubation results (see section 3.5 below). Easily available NH_4Cl-P, metal oxide-bound NaOH-SRP, and refractory residual were very low.

P-fractionation and subsequent analysis of metals of the 40 cm sediment core from BA1 revealed more information about the deeper sediment chemistry (Fig, 7).The lowest P concentration was in the 38-40 cm, there was a larger concentration peak at 28-34 cm and a smaller peak at 7-5 cm (Fig. 7). The big P peak corresponds to the greatest NaOH-P concentration which indicates that the application of aluminium sulphate in the lake in 1987. This is also shown by a peak in NaOH-Al in the similar depths (Fig. 7B). This peak spans over 6 cm which is an indication of sediment recycling for a longer time. NH4Cl-P, BD-P and Residual-P significantly decreased with increasing depth while NaOH-P significantly increased with increasing depth (Fig. 7, Table 2). BD-Fe concentration was very low (<0.1 mg g^{-1}) and was more or less uniform from 28 cm to the surface (Fig. 7). The bottom most layers have a lower calcium concentration and there is 3-fold increase in calcium at the surface sediments. The P concentrations in the extracts was positively correlated to the following elements P in each fraction (Table 2); NH_4Cl-P (to Ca and Mn); BD-P (to Mn), NaOH-P (to Al and Mn) and HCl-P (to Ca and Mn). When we combined the NH4Cl+BD fractions we found that the NH4Cl+BD-P was positively correlated to Mn, LOI_{550}, and LOI_{950} (Table 2)

The NaOH-Al : (NH4Cl+BD)-P molar ratios increased with depth and ranged from 2 to 9 (Fig 7). NaOH-Al : NaOH-P molar ratios had a narrow range (3 to 7) and they decreased in the upper sediment layers (<13 cm) and also in the sediment depth 26-32 cm (Fig. 7). The (NH4Cl-P, BD-P NaOH) Sum-Al : Sum-Fe was generally higher in the sediment below 15 cm in comparison to the sediment above; the difference was 2-3 fold (Fig. 7). The NaOH-Al : (NH4Cl + BD)-Fe molar ratio increased with depth and ranged between 5 and 51 and 7 to 37 respectively (Fig. 7). NaOH-Al : (NH4Cl + BD)-Mn molar ratio widely resembled the changes of NaOH-Al with depth (Fig 7b, lower panel); i.e. it increased with depth until 26 cm and decreased again from 34 to 40 cm sediment depth.

3.3 Solute fluxes from incubation experiments

Conditions during the incubation were maintained at the prescribed values for each treatment. Oxic treatments were kept oxic (> 95 % oxygen saturation) and anoxic treatments

were kept anoxic (< 2.5% oxygen saturation oxygen) over the course of the whole laboratory experiment (Table 3). Redox potential remained relatively high for anoxic-low temperature treatment despite the very low NO_3^- and oxygen concentration but became negative in anoxic-high temperature treatment, which also had a lower pH compared to other treatments (Table 3).

Phosphorus (SRP, DP, TP), NH_4^+-N, Fe, Mn decreased under oxic conditions (negative fluxes) and increased (positive fluxes) under anoxic conditions (Table 4). The opposite pattern emerged for NO_3^--N and SO_4^{2-}, which were rising under oxic conditions and diminished under anoxic conditions. DOC showed a decrease in three treatments (oxic-low temperature, oxic-high temperature, anoxic-low temperature) but increased in the anoxic high temperature treatment. Oxygen consumption for the high temperature oxic treatments was twice as high as in the low temperature oxic treatment.

Incubations clearly showed that sediment-borne P could only be released under anoxic conditions while under oxic conditions the sediment was even a sink for SRP. Temperature increase from 6°C to 20°C led to a five-fold higher SRP release rates under anoxic conditions, which for the entire lake resulted in a total mass flux of approximately 30 kg d^{-1}. Temperature is a major influencing factor for P-release from sediments of Lake Barleber.

Most of the fluxes for the treatments; oxic-low temperature, oxic-high temperature, anoxic-low temperature were not significantly different from zero based on t-test (Table 4). All of measured fluxes for the anoxic-high temperature treatment were significantly different from zero except for Fe. There was a significant difference between treatments ($p < 0.05$) for all fluxes except Fe flux (Table S1). Tukey HSD post hoc test confirmed that anoxic high temperature treatment was significantly different to at least one of the other treatments, with the exception of Mn (Table S1).

4. Discussion

4.1 Longevity of Al treatment

Lake Barleber is a special case of a relatively young gravel extraction lake (~90 years). It was successfully remediated for about 29 years before we sampled the sediment and remained with low total P until 2017, in comparison to the mean treatment longevity of about 11 years for lakes treated with aluminium (Huser et al. 2016). The main factors influencing longevity of water quality improvements after Al treatment are Al dose/area, hydraulic residence time, and Osgood morphological index (Huser et al. 2016). An aluminium treatment dosage of 36 g Al m^{-2} was applied to Lake Barleber. The lake water has a residence time of 10 years (Hannappel and Strom 2020) and an Osgood Index of 6.6. The magnitude of these factors are in agreement with the findings of (Huser et al. 2016), i.e., Al dose ≥ 15.1 g Al m^{-2}, high residence time, and Osgood Index > 5.7. Lake Barleber however does not meet the upper Al dose of 44.7 g Al m^{-2} observed by (Huser et al. 2016) for lakes with similar or higher treatment longevity. In addition, sedimentation rate might play an important role in treatment longevity; we hypothesize that lakes with lower sedimentation are likely to have longer treatment effectiveness due to the longer exposure of the aluminium layer to the water column i.e. limited aluminium burial.

Lake Barleber is a closed lake with no surface inflows and has a low inflow of groundwater; therefore, internal mobilization of nutrients from sediments into water are a predominant source of nutrients; in addition, lakes with long residence times are generally mostly influenced by internal processes (Huser et al. 2016). Monitoring data and incubation results point to the influence of temperature and dissolved O_2 as the major cause of the excessive nutrients release. Monitoring data also clearly showed that elevated temperatures and low O_2 concentration coincided with release of nutrients starting in autumn 2016 (Fig. 2). The effect of temperature and low oxygen on nutrient release is well known (Gudasz et al. 2010, Jensen and Andersen 1992); temperature affects mineralization processes and increase oxygen uptake leading to anoxia.

We also postulate, from the water chemistry data in April 2017, that immobilization of nutrients into the sediment in winter of 2016/17 did not take place or was insufficient to reduce nutrient levels to those similar to previous years. This is confirmed by data collected in the winter of 2018/2019 when a winter diatom bloom (triggered by temperature and light intensity under ice cover) occurred (peak chlorophyll *a* concentration of 93.4 $\mu g \cdot L^{-1}$) causing a reduction of the SRP concentration in the water column from 337 to 242 µg L^{-1} and Si from 1.55 to 0.05 mg L^{-1} (Kong et al. 2021). It is not known if winter diatom blooms occur every year but it is clear that their occurrence has a huge bearing on nutrient concentrations and

phytoplankton succession in spring as internal stores of P within the algal biomass can be quickly recycled into the SRP pool once the algal bloom is mineralized.

4.2 Phosphorus release was predominantly redox-dependent

Our results provide consistent evidence that redox-dependent P release was the major process responsible for P release in Lake Barleber during summer; this classical P release model is well known from literature (Einsele 1936, Jensen and Andersen 1992, Mortimer 1942, Nürnberg 2020, Nürnberg et al. 2012). However Mn seems to be the major element binding P; the correlation of the (NH4Cl + BD)-P to (NH4Cl + BD)-Fe was low and insignificant. We think Fe is immobilized by sulphides hence the poor correlation; this implies that Mn may be a better indicator of redox-dependent P release in lakes with a high sulphide content. We also observed significant correlation of (NH4Cl + BD)-P with LOI_{550} (proxy for organic matter content) and LOI_{950} (proxy for calcium carbonates) which implies that organic matter content and calcium carbonates play a role in the in mobilization and immobilization of P.

Nutrients fluxes were highest under the anoxic-high temperature conditions. This shows that besides low redox potential also high temperatures enhance release of nutrients (Jensen and Andersen 1992, Dadi et al. 2020) as shown by the correlations above. Thus, redox-potential and temperature work here synergistically and are major drivers of eutrophication. Lake warming indeed played a role, a recent study shows that internal loading and lake warming explains 68% and 32% of the blooms respectively (Kong et al. 2023). The self-amplifying mechanisms between high temperature and low redox conditions are multiple: (i) high temperature accelerate oxygen depletion and hence rapidly induce low redox conditions, (ii) high temperatures also amplify mineralization (Gudasz et al. 2010) and thus support nutrient recycling, (iii) high temperatures induce a shift towards cyanobacteria (Paerl and Huisman 2008) that have a high potential for bloom-formation and such a shift comes along with low phosphorus sedimentation (Horn et al. 2015). Once a lake becomes eutrophic, as what happened to Lake Barleber in 2016, there are also self-stabilizing mechanisms at play given that the higher algal biomasses lead to higher sediment oxygen demand and a phosphorus accumulation at the sediment surface. It is therefore not surprising that the algal bloom in 2016 stimulated bloom formation and a further increase in epilimnetic SRP concentration in the summer of 2017; similar positive feedback mechanism of algal blooms have been observed in Lake Taihu (Qin et al. 2021). The algal bloom that followed the SRP release resulted in notable changes in the upper sediment layer i.e. the PN and POC in the upper sediment were higher than in the lower sediment layers, most probably due to the rapid change in sediment composition after only one vegetative season. The senescence of algal

blooms led to an increase in easily mobilized P sources (NH_4Cl-P and BD-P) in the upper layers.

4.3 Sediment P adsorption capacity

The TP concentration in the upper 5 cm of the sediment in August 2017 was 3 times higher (3.4 mg P g^{-1}) than the other four cores (1 mg P g^{-1}). The TP concentration of four cores is on the lower end of the scale in other lakes; up to 7 mg P g^{-1} with an average of approximately 2 mg P g^{-1} (Hupfer 1995). The higher concentration observed in August 2017 could be either due to sediment focusing at the particular point and/or calcite precipitation which has been observed in the lake in 2018 and has been attributed to algal blooms which raised pH to almost 10 (Seewald, 2019). The calcite precipitation would have been driven by increased pH level in the lake due to the algal bloom (Leiser et al. 2021).

The relatively low sediment TP concentration in Lake Barleber can also be interpreted as an indication of limited P adsorption capacity. Release of redox-dependent P requires a larger pool of sedimentary P adsorbed to iron minerals, which compete with Al for adsorbing P. Aluminum treatment of lakes shifts this balance towards Al minerals, whose adsorption of P is insensitive to redox conditions. Our results indicate that in Lake Barleber the P-fraction adsorbed to redox-sensitive metal hydroxides was relatively high and this was probably due to reduced P adsorption capacity of the sediment as a result of aging Al minerals (Berkowitz et al. 2006).

We estimated the P retention by calculating various molar ratios commonly used as proxies for P retention (Huser 2017, Kopáček et al. 2005, Nürnberg et al. 2018, Rydin and Welch 2000). The NaOH-Al : NaOH-P molar ratio was 3 at depth between 30 and 34 cm and it increased to about 6 then started to decrease to 4 or 5 in the upper sediment; the whole sediment column has NaOH-Al : NaOH-P molar ratios below the thresholds of 10 and 12.6 proposed by Rydin and Welch (2000) and de Vicente et al. (2008), respectively. The NaOH-Al : NaOH-P ratios are however mostly within the range of 2 to 100 like observed in other lake sediments (de Vicente et al. 2008, Huser 2017, Nürnberg et al. 2018). The NaOH-Al: (NH4Cl + BD)-P molar ratio was 7 after Al treatment and decreased to 3 in the upper sediment; the ratios are far below the proposed threshold of >25 (Kopáček et al. 2005). The sum-Al : sum-Fe ratio (NH4Cl + BD + NaOH) was higher at the time of Al application and decreased 5 fold approaching the >3 threshold proposed by Kopáček et al. (2005). This is one ratio that seems to explain clearly the loss of P retention in the Lake Barleber sediments over time. NaOH-Al : (NH4Cl + BD)-Fe and NaOH-Al : (NH4Cl + BD)-Mn molar ratios also clearly show the deceasing P retention capacity in the sediment over time, however the Fe ratios have more noise. The noise of the NaOH-Al : (NH4Cl + BD)-Fe molar ratios could be due to different rates of immobilization of Fe by sulphides formed as a result of sulphate

reduction. The NaOH-Al : (NH4Cl + BD)-Fe ratios have a clear trend which also enables the identification Al peak at depth between 28 and 34 cm. Most of the molar ratios in literature are from short term laboratory experiments or lakes which have been recently treated (<3 years), this makes it difficult to compare the results of Lake Barleber to other studies.

The ratios increase with depth because the influence of the aluminum treatment is diminished upward in the sediment due to sedimentation of material with a lower P binding capacity. Lake Barleber has a high background sulphate concentration; before the treatment in 1986, the sulphate concentration was ca. 500 mg L^{-1} and it increased to ca. mg L^{-1} after the aluminium sulfate treatment (Rönicke and Bahr 1989). In addition, phosphorus sorption capacity by aluminum decreases with time (Anderson and Berkowitz 2010, Berkowitz et al. 2005); thus, adsorption sites might have been saturated because of 30 years of aging. Al is transformed from a poorly-ordered amorphous solid phase to a well-ordered gibbsite and this polymerization reduces surface area i.e. Al floc sorption capacity for phosphate decreases over time (Berkowitz et al. 2006, James 2017, Kopáček et al. 2005).

Another factor which contributed to reduced adsorption capacity of the sediments is the high concentration of sulphate and potential sulphate reduction. This can lead to formation of sulphides which permanently immobilize the reduced iron released under anoxia through formation of iron sulphides thereby leading to a reduction of the active iron pool (Gachter and Muller 2003). All this compromise the duration of the treatment effectiveness hence the need for a monitoring of the sediment geochemistry and potential treatment, again. Based on this observation we would recommend that lake managers apply poly-aluminum chloride instead of aluminum sulphate.

4.4 Sediment susceptibility to resuspension and focusing

Sediment NaOH-Al revealed there is an Al peak in the sediment (28-34 cm sediment depth) which is likely due to the Al treatment in 1986. The peak is not high which could be due to a high background Al concentration in the sediment in comparison to the amount added during remediation as shown by another study (Lewandowski et al. 2003) or due to sediment re-suspension/re-working. The thickness of the Al peak layer is likely an indication of sediment focusing to the deepest area (sampling point BA1). If we take 28 cm depth as the marker for 1986 Al treatment, this implies an average sediment accumulation rate of 0.9 cm per year which is three times higher than the mean for lakes of 0.3 cm y^{-1} (Baud et al. 2021). It is therefore plausible that sediment focusing occurs in Lake Barleber. Aluminum flocs formed after the application of Al are light enough to be resuspended by wind or benthivorous fish as shown in other studies (Egemose et al. 2013). A study on macrophytes in Lake Barleber indeed revealed relatively high activity of benthivorous fish which would explain the sediment re-distribution (Lana plan 2016). In addition, the sediment dry density in the upper sediment

is distinctly lower in comparison to the deeper sediments. This is expected since Lake Barleber is a closed lake and sedimentation is predominantly from autochthonous material, which has a lower dry density and is highly susceptible to resuspension. Sediment susceptibility to resuspension increases with decreasing dry density of sediment layers (Jepsen et al. 1997). We postulate that low sedimentation prolongs the duration of the treatment effectiveness because a thin layer of fresh sediment can easily be mixed into the Al rich sediment layer i.e. the Al rich layer is not completely buried but is rather mixed with new sediment, as observed. This is probably what happened in Lake Barleber which would imply that the treatment longevity is supported by the presumably low sedimentation rate in the lake due to the low productivity in the lake. The quite gradual decrease of the NaOH-Al (Fig 7b, lower panel) supports our interpretation that sediment resuspension and focusing is a permanent feature of Lake Barleber.

4.5 Phosphorus quantity in water and sediment

Lake-wide TP in Lake Barleber in the time period from 1987 (after aluminum treatment) until 2014 showed amounts between 173 and 373 kg TP and the average amount was approximately 258 kg TP (Fig. 8). Based on water sampling in 2017 the total TP amount in Lake Barleber notably increased 8-fold and reached values of approximately 2160 kg. This implies that from 2014 to 2017 approximately 1900 kg TP were mobilized from the sediments. Given a lake sediment surface area of 103 ha this translates to a flux rate of 0.6 g P m^{-2} $year^{-1}$ (633 kg $year^{-1}$). Anoxic incubation flux was 0.37 g P m^{-2} $year^{-1}$ (381 kg $year^{-1}$). The P flux rate from sediment incubation is therefore an underestimation of the actual flux given that atmospheric deposition, groundwater and bathing are low (Rinke et al. 2018). This underestimation may be due to sediment heterogeneity since the sediment incubation was from one sampling point. Estimated TP content of 633 kg $year^{-1}$ is ten times higher than total external P load of 65 kg $year^{-1}$ i.e. atmospheric deposition, groundwater and bathing (Hannappel and Strom 2020, Rinke et al. 2018). Interestingly the TP content of 633 kg $year^{-1}$ is very similar to the mean BD-P content of 790 kg in the upper 1 cm sediment layer (Fig. 6). This shows that most of the redox dependent P in the upper 1 cm layer was remobilized into the water column. It is therefore clear that internal P loading was the source of the observed increase in P concentration.

4.6. Potential mechanism for the sudden phosphorus release

Lake Barleber is a classic example of a lake in which P release is controlled by redox sensitive metal hydroxides and hence the application of redox insensitive Al was successful in controlling P release for approximately 30 years. The lake is more prone to sediment mixing in the upper sediment layers; we presume that sedimentation prior to the algal blooms was low (closed lake). This could explain why Al treatment was successful; after the Al

application the aluminum- rich layer continued to be recycled via resuspension hence continuous adsorption of P for a long time unlike in high sedimentation systems where this layer can quickly get buried and become inaccessible. The autochthonous sedimentation also leads to a decrease in dry density and this, coupled with a potential decrease in Al sorption capacity (due to aging), led to a start of the tipping (Fig. 9) towards re-eutrophication. The lake became highly susceptible to anoxia, especially considering the high BD-P fraction of associated with the redox-dependent hydroxides and decrease in the P retention as molar ratios (Fig. 7). Post-treatment monitoring of sediment P fractionation in the upper 5 cm is important to determine the extent to which the sediment loses its permanent Al adsorption capacity for P.

5. Conclusion

We have shown that internal loading can explain the shift towards eutrophy in a lake previously treated with aluminum sulphate. The study also confirms the role of anoxia and high water temperatures (mineralization of organic matter) as the major drivers of P-release. After release the P stimulates algae leading to self-sustaining algal blooms, i.e., large P-pools are within the algal biomasses (during blooms in winter and summer) and are quickly recycled into the water before P is permanently sequestered in the sediment.

This is a study that analyzed nutrient dynamics in lakes that had been treated with aluminum sulfate three decades before eutrophic conditions returned. We identified key mechanisms that finally lead to a eutrophic condition and provide evidence that many treated lakes at some time will require additional treatment for sustaining acceptable water quality. There is need for more long term studies on the sediment in aluminum treated lakes especially on the long term aging of Al precipitates. Development and application of a method for measuring the remaining P-binding capacity of the sediment and/or the Al precipitates is required for the management of aluminum treated lakes.

Acknowledgements

We thank Burkhard Kuehn, Michael Herzog, Rebecca Lellau Karsten Rahn, and Martin Wieprecht for the sampling. We also thank the members of the UFZ Laboratory for Water Analytics & Chemometrics (GEWANA): Heike Goreczka, Andrea Hoff, Dorothee Ohlwein, and Ina Siebert for the analysis of samples. We thank the Landesbetrieb für Hochwasserschutz und Wasserwirtschaft Sachsen-Anhalt (LHW) for the historical monitoring data. We also thank Gertrud Nürnberg and an anonymous reviewer for their detailed and thorough reviews which improved this manuscript a lot.

Funding

This research did not receive any specific grant from funding agencies in the public, commercial, or not-for-profit sectors.

References

Anderson, M.A. and Berkowitz, J. (2010) Aluminum polymers formed following alum treatment of lake water. Chemosphere 81(7), 832-836.

Bauch, G., 1953. Der Barleber See. Mitteilungen für Naturkunde und Vorgeschichte(Lake Barleber. Communications for natural history and prehistory). Aus dem Museum für Kulturgeschichte in Magdeburg 3, 173-183

Baud, A., Jenny, J.-P., Francus, P. and Gregory-Eaves, I. (2021) Global acceleration of lake sediment accumulation rates associated with recent human population growth and land-use changes. Journal of Paleolimnology 66(4), 453-467.

Berkowitz, J., Anderson, M.A. and Amrhein, C. (2006) Influence of aging on phosphorus sorption to alum floc in lake water. Water Research 40(5), 911-916.

Berkowitz, J., Anderson, M.A. and Graham, R.C. (2005) Laboratory investigation of aluminum solubility and solid-phase properties following alum treatment of lake waters. Water Research 39(16), 3918-3928.

Dadi, T., Rinke, K. and Friese, K. (2020) Trajectories of Sediment-Water Interactions in Reservoirs as a Result of Temperature and Oxygen Conditions. Water 12(4).

Dadi, T., Völkner, C. and Koschorreck, M. (2015) A sediment core incubation method to measure the flux of dissolved organic carbon between sediment and water. Journal of Soils and Sediments 15(12), 2350-2358.

de Vicente, I., Huang, P., Andersen, F.Ø. and Jensen, H.S. (2008) Phosphate Adsorption by Fresh and Aged Aluminum Hydroxide. Consequences for Lake Restoration. Environmental Science & Technology 42(17), 6650-6655.

Egemose, S., Reitzel, K., Andersen, F.Ø. and Jensen, H.S. (2013) Resuspension-mediated aluminium and phosphorus distribution in lake sediments after aluminium treatment. Hydrobiologia 701(1), 79-88.

602 Einsele, W. (1936) Ueber die Beziehungen des Eisenkreislaufs zum
603 Phosphatekreislauf im eutrophen See. Archiv Fur Hydrobiologie 29, 664–686.

604 Foy, R.H. (1985) Phosphorus inactivation in a eutrophic lake by the direct addition of
605 ferric aluminium sulphate: impact on iron and phosphorus. Freshwater Biology
606 15(5), 613-629.

607 Friese, K., Schultze, M., Boehrer, B., Büttner, O., Herzsprung, P., Koschorreck, M.,
608 Kuehn, B., Rönicke, H., Tittel, J., Wendt-Potthoff, K., Wollschläger, U., Dietze,
609 M. and Rinke, K. (2014) Ecological response of two hydro-morphological
610 similar pre-dams to contrasting land-use in the Rappbode reservoir system
611 (Germany). International Review of Hydrobiology 99(5), 335-349.

612 Gachter, R. and Muller, B. (2003) Why the phosphorus retention of lakes does not
613 necessarily depend on the oxygen supply to their sediment surface. Limnology
614 and Oceanography 48(2), 929-933.

615 Gudasz, C., Bastviken, D., Steger, K., Premke, K., Sobek, S. and Tranvik, L.J. (2010)
616 Temperature-controlled organic carbon mineralization in lake sediments.
617 Nature 466(7305), 478-U473.

618 Hannappel, S. and Strom, A. (2020) Methode zur Ermittlung des Phosphoreintrags
619 über das Grundwasser in den Barleber See bei Magdeburg (Method to
620 determine the amount of phosphorous entering Barleber See near Magdeburg
621 via groundwater). Korrespondenz Wasserwirtschaft 13(1).

622 Horn, H., Paul, L., Horn, W., Uhlmann, D. and Röske, I. (2015) Climate change
623 impeded the re-oligotrophication of the Saidenbach Reservoir. International
624 Review of Hydrobiology 100(2), 43-60.

625 Hupfer, M. (1995) Handbuch Angewandte Limnologie. Steinberg, C., Bernhard, H.
626 and Klapper, H. (eds), Ecomed, Landsberg/Lech.

627 Huser, B.J., Egemose, S., Harper, H., Hupfer, M., Jensen, H., Pilgrim, K.M., Reitzel,
628 K., Rydin, E. and Futter, M. (2016) Longevity and effectiveness of aluminum
629 addition to reduce sediment phosphorus release and restore lake water
630 quality. Water Research 97(Supplement C), 122-132.

631 Huser, B.J. (2017) Aluminum application to restore water quality in eutrophic lakes:
632 maximizing binding efficiency between aluminum and phosphorus. Lake and
633 Reservoir Management 33(2), 143-151.

634 James, W.F. (2017) Phosphorus binding dynamics in the aluminum floc layer of Half
635 Moon Lake, Wisconsin. Lake and Reservoir Management 33(2), 130-142.

636 James, W.F. and Bischoff, J.M. (2019) Sediment aluminum:phosphorus binding
637 ratios and internal phosphorus loading characteristics 12 years after aluminum
638 sulfate application to Lake McCarrons, Minnesota. Lake and Reservoir
639 Management, 1-13.

640 Jarvie, H.P., Johnson, L.T., Sharpley, A.N., Smith, D.R., Baker, D.B., Bruulsema,
641 T.W. and Confesor, R. (2017) Increased Soluble Phosphorus Loads to Lake
642 Erie: Unintended Consequences of Conservation Practices? Journal of
643 Environmental Quality 46(1), 123-132.

644 Jensen, H.S. and Andersen, F.O. (1992) Importance of temperature, nitrate, and pH
645 for phosphate release from aerobic sediments of four shallow, eutrophic lakes.
646 Limnology and Oceanography 37(3), 577-589.

647 Jeppesen, E., Søndergaard, M., Jensen, J.P., Havens, K.E., Anneville, O., Carvalho,
648 L., Coveney, M.F., Deneke, R., Dokulil, M.T., Foy, B., Gerdeaux, D., Hampton,
649 S.E., Hilt, S., Kangur, K., Köhler, J., Lammens, E.H.H.R., Lauridsen, T.L.,
650 Manca, M., Miracle, M.R., Moss, B., Nõges, P., Persson, G., Phillips, G.,
651 Portielje, R., Romo, S., Schelske, C.L., Straile, D., Tatrai, I., Willén, E. and
652 Winder, M. (2005) Lake responses to reduced nutrient loading – an analysis of
653 contemporary long-term data from 35 case studies. Freshwater Biology
654 50(10), 1747-1771.

655 Klapper, H. and Geller, W. (2001) Water Quality Management of Mining Lakes — a
656 New Field of Applied Hydrobiology. Acta Hydrochimica et Hydrobiologica 29(6-
657 7), 363-374.

658 Kong, X., Seewald, M., Dadi, T., Friese, K., Mi, C., Boehrer, B., Schultze, M., Rinke,
659 K. and Shatwell, T. (2021) Unravelling winter diatom blooms in temperate
660 lakes using high frequency data and ecological modeling. Water Research
661 190, 116681.

662 Kong, X., Determann, M., Andersen, T.K., Barbosa, C.C., Dadi, T., Janssen, A.B.G.,
663 Paule-Mercado, M.C., Pujoni, D.G.F., Schultze, M. and Rinke, K. (2023)
664 Synergistic Effects of Warming and Internal Nutrient Loading Interfere with the
665 Long-Term Stability of Lake Restoration and Induce Sudden Re-
666 eutrophication. Environmental Science & Technology.

667 Kopáček, J., Borovec, J., Hejzlar, J., Ulrich, K.-U., Norton, S.A. and Amirbahman, A.
668 (2005) Aluminum Control of Phosphorus Sorption by Lake Sediments.
669 Environmental Science & Technology 39(22), 8784-8789.

670 Lana plan (2016) Erhebung von Makrophyten und Diatomeen in Seen Sachsen-
671 Anhalts (Survey of macrophytes and diatoms in lakes of Saxony-Anhalt).
672 Unpublished report of lana plan GbR (Nettetal, Germany) to Landesbetrieb für
673 Hochwasserschutz und Wasserwirtschaft Sachsen-Anhalt (Magdeburg,
674 Germany)

675 Leiser, R., Jongsma, R., Bakenhus, I., Möckel, R., Philipp, B., Neu, T.R. and Wendt-
676 Potthoff, K. (2021) Interaction of cyanobacteria with calcium facilitates the
677 sedimentation of microplastics in a eutrophic reservoir. Water Research 189,
678 116582.

679 Lewandowski, J., Schauser, I. and Hupfer, M. (2003) Long term effects of
680 phosphorus precipitations with alum in hypereutrophic Lake Süsser See
681 (Germany). Water Research 37(13), 3194-3204.

682 LHW, Landesbetrieb für Hochwasserschutz und Wasserwirtschaft Sachsen-Anhalt
683 (2020), Monitoringergebnisse der vergangenen Jahre (Monitoring results of
684 the previous years). Website (https://lhw.sachsen-anhalt.de/untersuchen-
685 bewerten/monitoringergebnisse/ accessed 11.08.2020).

686 Lürling, M. and Oosterhout, F.v. (2013) Controlling eutrophication by combined bloom
687 precipitation and sediment phosphorus inactivation. Water Research 47(17),
688 6527-6537.

689 Mesman, J.P., Stelzer, J.A.A., Dakos, V., Goyette, S., Jones, I.D., Kasparian, J.,
690 McGinnis, D.F. and Ibelings, B.W. (2021) The role of internal feedbacks in
691 shifting deep lake mixing regimes under a warming climate. Freshwater
692 Biology 66(6), 1021-1035.

693 Mollema, P.N. and Antonellini, M. (2016) Water and (bio)chemical cycling in gravel pit
694 lakes: A review and outlook. Earth-Science Reviews 159, 247-270.

695 Morgenstern, P., Friese, K., Wendt-Potthoff, K. and Wennrich, R. (2001) Bulk
696 Chemistry Analysis of Sediments from Acid Mine Lakes by Means of
697 Wavelength Dispersive X-ray Fluorescence. Mine Water and the Environment
698 20(3), 105-113.

699 Mortimer, C.H. (1942) The exchange of dissolved substances between mud and
700 water in lakes. Journal of Ecology 30(1), 147-201.

701 Nürnberg, G.K., Tarvainen, M., Ventelä, A.-M. and Sarvala, J. (2012) Internal
702 phosphorus load estimation during biomanipulation in a large polymictic and
703 mesotrophic lake. Inland Waters 2(3), 147-162.

704 Nürnberg, G.K., Fischer, R. and Paterson, A.M. (2018) Reduced phosphorus
705 retention by anoxic bottom sediments after the remediation of an industrial
706 acidified lake area: Indications from P, Al, and Fe sediment fractions. Science
707 of the Total Environment 626, 412-422.

708 Nürnberg, G.K. (2020) Internal Phosphorus Loading: Causes, case studies, and
709 management. Steinman, A.D. and Spears, B.M. (eds), J. Ross Publishing.

710 Osgood, R.A. (1988) Lake mixis and internal phosphorus dynamics.

711 Paerl, H.W. and Huisman, J. (2008) Blooms Like It Hot. Science 320(5872), 57-58.

712 Qin, B., Deng, J., Shi, K., Wang, J., Brookes, J., Zhou, J., Zhang, Y., Zhu, G., Paerl,
713 H.W. and Wu, L. (2021) Extreme Climate Anomalies Enhancing
714 Cyanobacterial Blooms in Eutrophic Lake Taihu, China. Water Resources
715 Research 57(7), e2020WR029371.

716 Rinke, K., Friese, K., Schultze, M., Rönicke, H., Lellau, R. and Dadi, T. (2018)
717 Entwicklung der Wasserqualität des Barleber Sees, Abschätzung der internen
718 Nährstoffbelastung und Handlungsempfehlungen für
719 Wassergüteverbesserungen (Development of the water quality of the Barleber
720 Lake, estimation of the internal nutrient load and recommendations for action
721 to improve the water quality). UFZ-Helmholtz Centre for Environmental
722 Research.

723 Rönicke H. and Bahr K. (1989) Nährstoffausfällung an einem Magdeburger Badesee
724 zur Verbesserung der Wasserbeschaffenheit und des Erholungswertes
725 (Nutrient precipitation at a Magdeburg bathing lake to improve water quality
726 and recreational value). Wasserwirtschaft-Wassertechnik 39:187-188)

727 Rönicke, H., Frassl, M.A., Rinke, K., Tittel, J., Beyer, M., Kormann, B., Gohr, F. and
728 Schultze, M. (2021) Suppression of bloom-forming colonial cyanobacteria by
729 phosphate precipitation: A 30 years case study in Lake Barleber (Germany).
730 Ecological Engineering 162, 106171.

731 Rydin, E. and Welch, E.B. (2000) Amount of phosphorus inactivated by alum
732 treatments in Washington lakes. Water Research 45, 226-230.

733 Seelen, L.M.S., Teurlincx, S., Armstrong, M.R., Lürling, M., van Donk, E. and de
734 Senerpont Domis, L.N. (2022) Serving many masters at once: a framework for
735 assessing ecosystem services delivered by quarry lakes. Inland Waters 12(1),
736 121-137.

737 Shatwell, T. and Köhler, J. (2019) Decreased nitrogen loading controls summer
738 cyanobacterial blooms without promoting nitrogen-fixing taxa: Long-term
739 response of a shallow lake. Limnology and Oceanography 64(S1), S166-S178.

740 Søndergaard, M., Jensen, J.P. and Jeppesen, E. (2005) Seasonal response of
741 nutrients to reduced phosphorus loading in 12 Danish lakes. Freshwater
742 Biology 50(10), 1605-1615.

743 Steinman, A., Rediske, R. and Reddy, K.R. (2004) The reduction of internal
744 phosphorus loading using alum in Spring Lake, Michigan. Journal of
745 Environmental Quality 33(6), 2040-2048.

746 Taranu, Z.E., Zurawell, R.W., Pick, F. and Gregory-Eaves, I. (2012) Predicting
747 cyanobacterial dynamics in the face of global change: the importance of scale
748 and environmental context. Global Change Biology 18(12), 3477-3490.

Figure captions

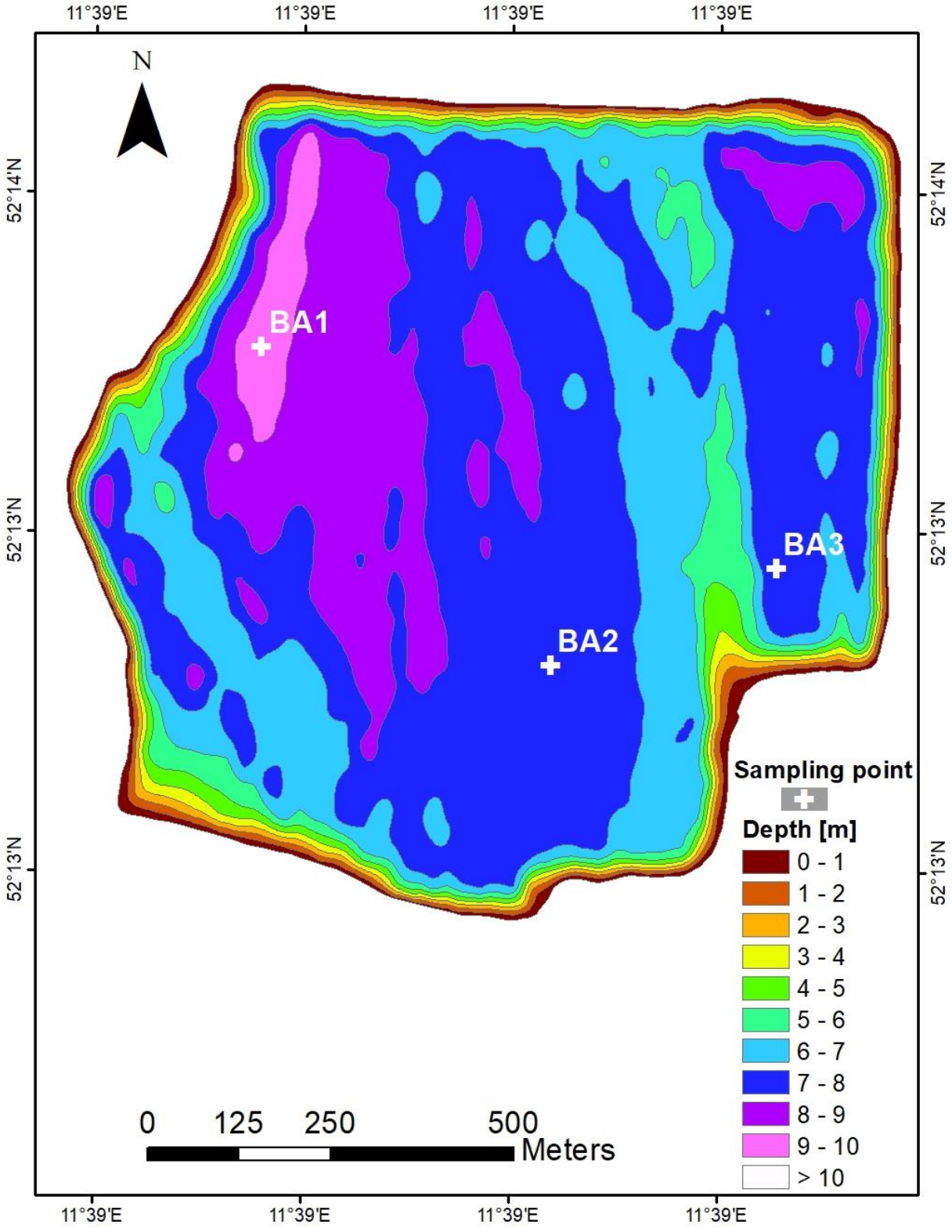

Fig 1 Bathymetric map of Lake Barleber, Germany showing the sampling sites (BA1, 2, & 3). Data source: Landesbetrieb für Hochwasserschutz und Wasserwirtschaft Sachsen-Anhalt (LHW).

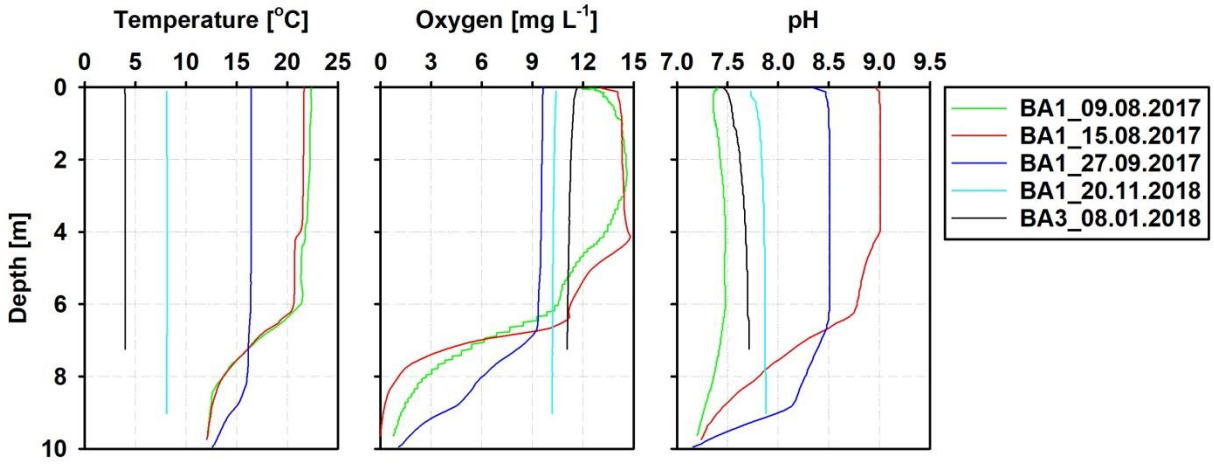

754

755 **Fig. 2. Oxygen and temperature profiles at the time of sediment sampling**

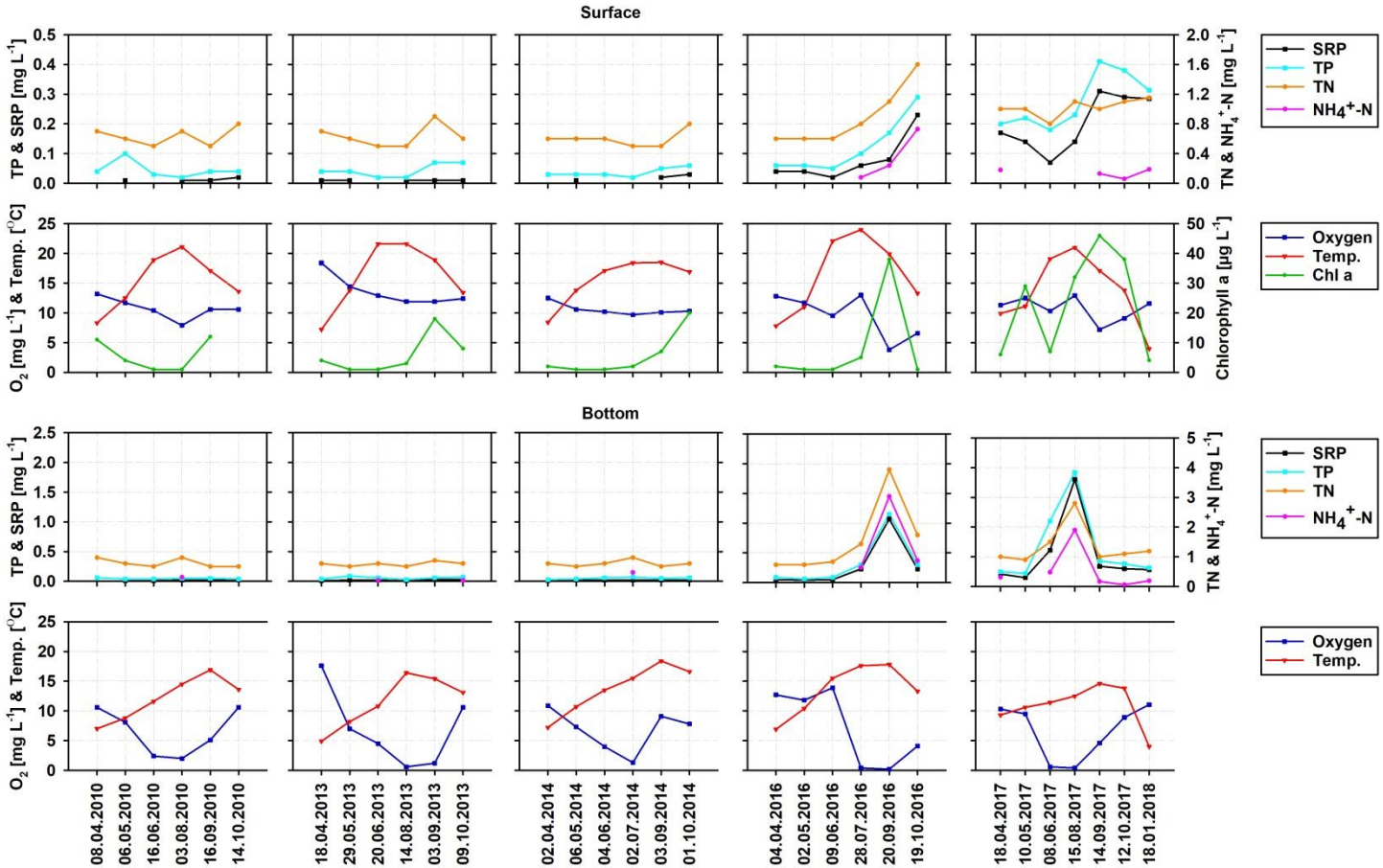

Fig. 3. Dynamics of nutrients, chlorophyll a, oxygen and temperature in the epilimnion and bottom part of the lake from 2010 to 2017. All dates without SRP and NH_4^+-N refer to values <0.01 and 0.02 mg L^{-1} respectively. The bottom SRP and TP concentration before 2016 were below 0.04 and 0.1 mg L^{-1} respectively. Data source (LHW, 2020). Please note, the epilimnion and bottom nutrients charts have different scales. The last data point 18.01.2018 is from this study.

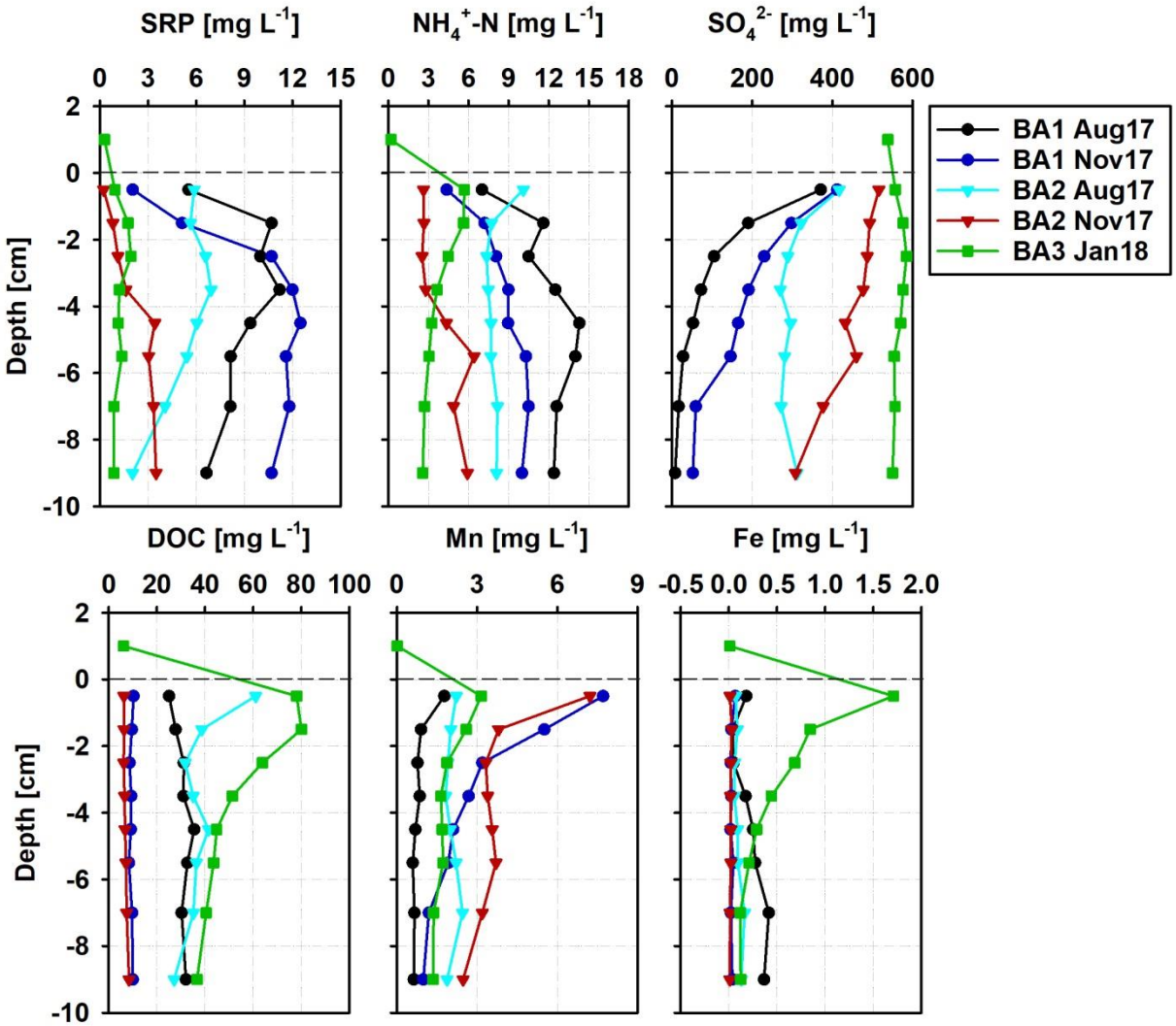

761

762 **Fig. 4. Porewater and overlying water (OW) solute concentrations**

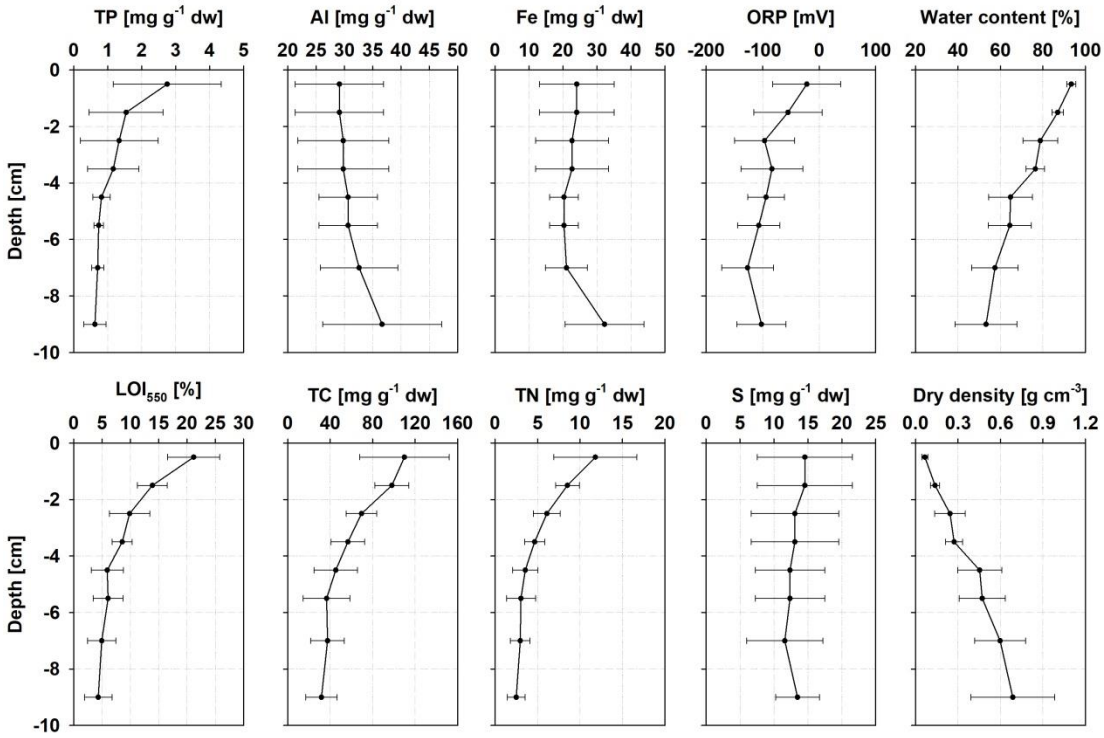

Fig. 5 Means of sediment parameters in the upper 10 cm sediment. The data are means of 5 sediment (n = 5) cores from 3 sampling points. The whiskers indicate the standard deviation

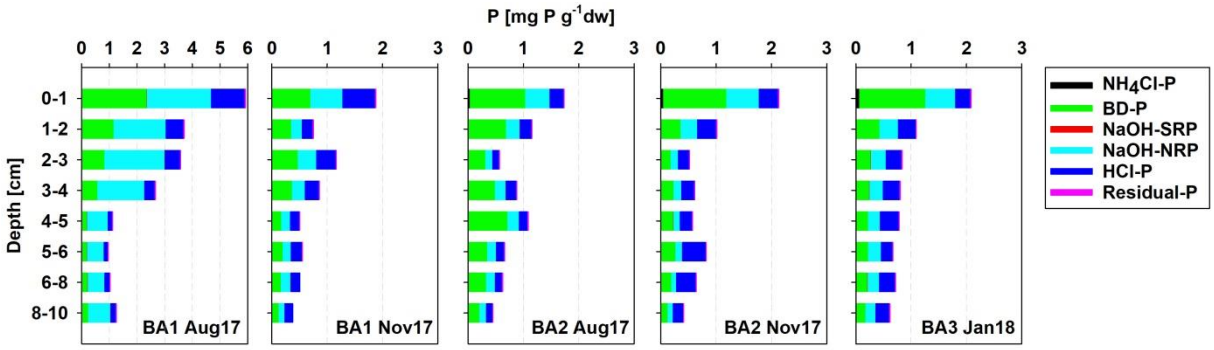

768

769 **Fig. 6. P-fractionation in the upper 10 cm for the three coring sites and at different**
770 **times.**

771

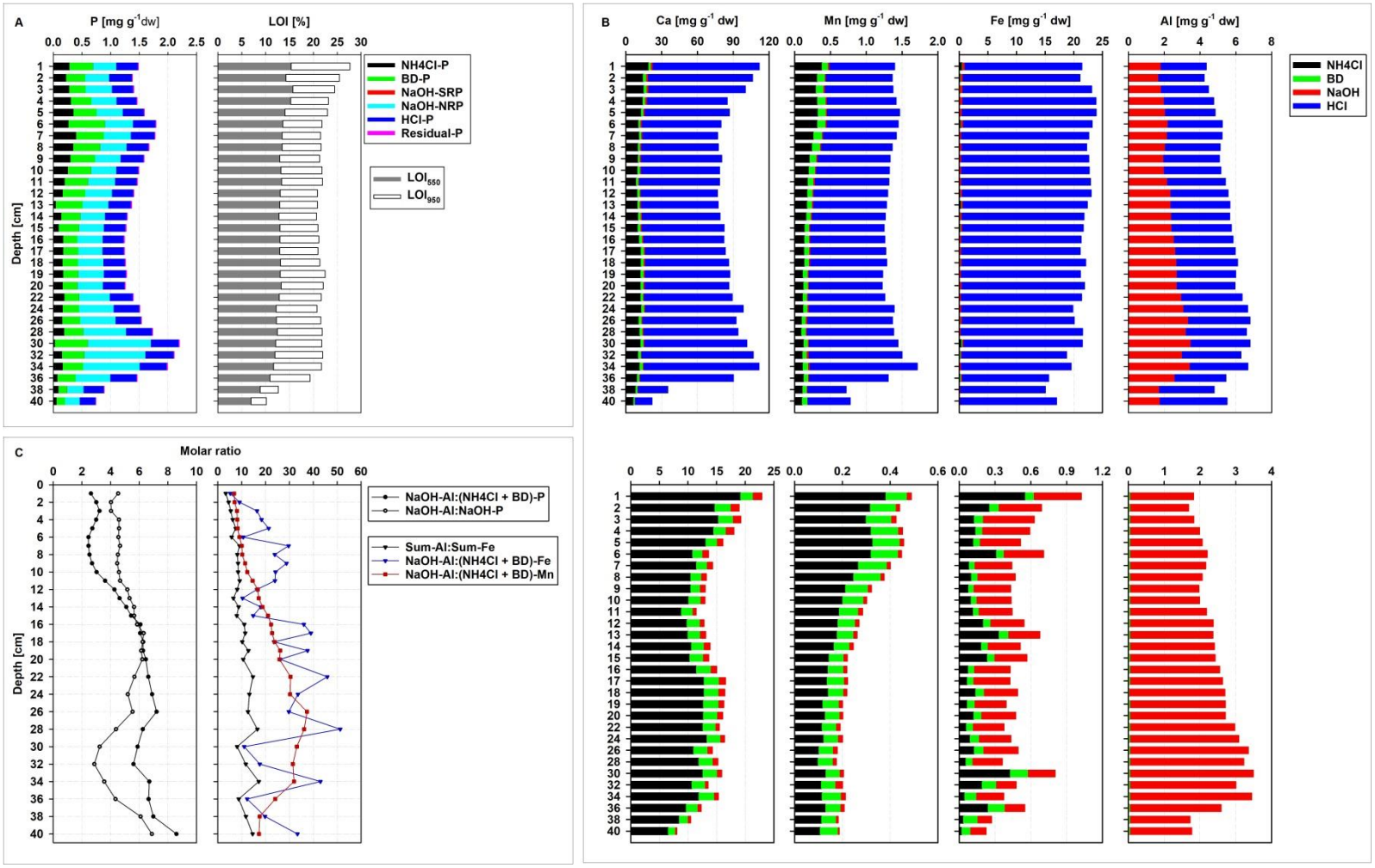

Fig. 7. P fractionation and loss on ignition (A), metal content in the fractionation extracts (B) and selected P retention indicators (C) of the 40cm sediment core from sampling point BA1.

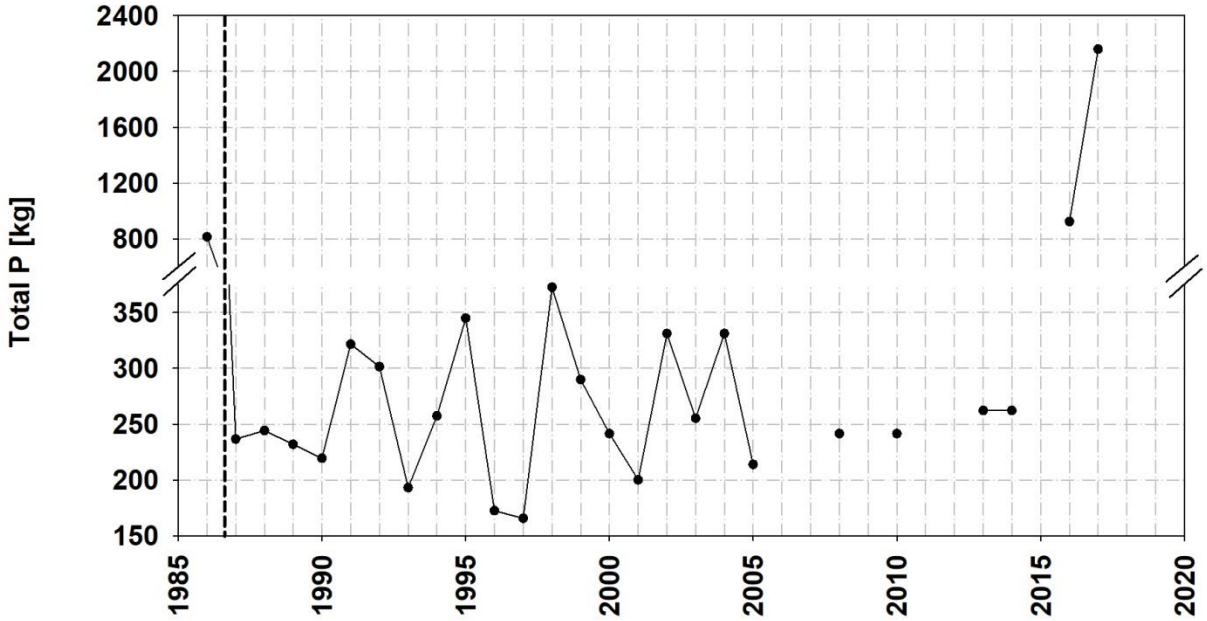

Fig. 8. Quantity of phosphorus in the open water of Lake Barleber: Based on long term concentration data from (Data Source: Roenicke et al. 1995; unpublished data of UFZ; data of LHW). The black vertical dotted black line indicates the aluminum sulfate treatment in 1986. Please note the break in the y-axis.

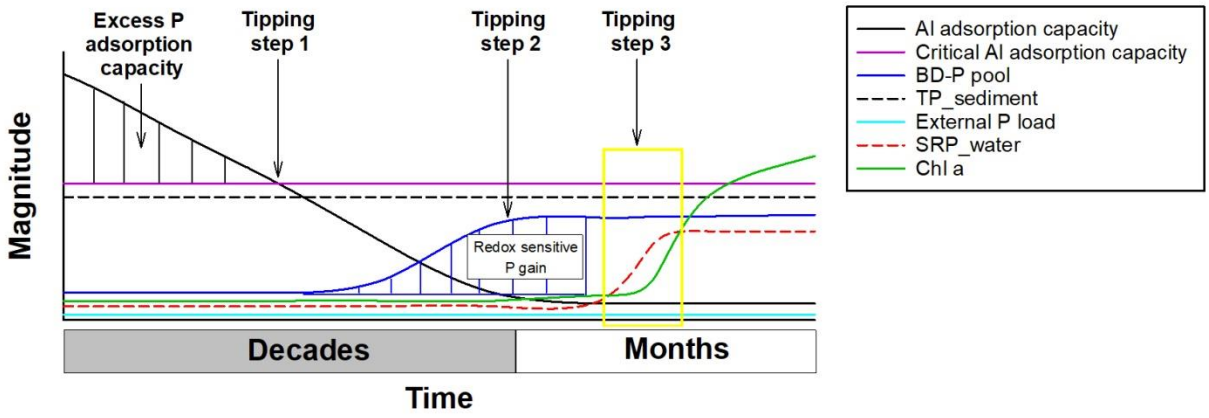

Fig 9 A conceptual model of the loss of Al adsorption capacity for P and the accumulation of available P after remediation with aluminum sulphate. Tipping (shift towards P release) starts when the Al adsorption capacity is not adequate to bind the non-bound P below the critical threshold (step 1). This is followed by an increase in the BD-P capacity since the P that was bound by Al becomes available to Mn and Fe (step 2). Once the BD-P pool reaches the maximum the system becomes very vulnerable to high temperature and anoxia leading to events like wind mixing to transport P to the epilimnion where the phytoplankton bloom occurs (step 3). This model applies to closed lakes with minimal groundwater and atmospheric P deposition influence.

Tables

Table 1. Lake Barleber mean nutrients concentrations in the epilimnion and bottom part of the lake (parentheses); before and after re-eutrophication. Data source: (LHW 2020).

Nutrients	Before	After	
	2013 – 2014 (n = 12)	**2016 (n = 6)**	**2017 (n = 6)**
TP [µg L^{-1}]	40 ± 18	122 ± 86	270 ± 90
	(55 ± 17)	(332 ± 379)	(717 ± 613)
TN [mg L^{-1}]	0.63 ± 0.12	0.88 ± 0.37	1 ± 0.1
	(0.62 ± 0.08)	(1.43 ± 1.12)	(1.38 ± 0.66)
Chlorophyll *a* [µg L^{-1}]	5.67 ± 6.38	9.40 ± 14.37	26.33 ± 15.00

Table 2. Significant correlations (Pearson) of the parameters in the fractionation extracts of the 40cm sediment core from sampling point BA1; n = 30, α =0.05

Parameter	r	p
NH_4Cl-P vs Depth	-0.72	$6.54e^{-6}$
BD-P vs Depth	-0.45	0.013
NaOH-P vs Depth	0.42	0.021
Residual-P vs Depth	-0.38	0.036
NH_4Cl: P vs Ca	0.41	0.025
NH_4Cl: P vs Mn	0.72	$5.77e^{-6}$
BD: P vs Mn	0.46	0.01
NaOH: P vs Mn	0.57	0.001
NaOH: P vs Al	0.76	$9.78e^{-7}$
HCl: P vs Ca	0.74	$3.38e^{-6}$
HCl: P vs Mn	0.83	$1.76e^{-8}$
(NH_4Cl + BD): P vs Mn	0.75	$1.5e^{-6}$
(NH_4Cl + BD): P vs LOI_{550}	0.64	0.0001
(NH_4Cl + BD): P vs LOI_{950}	0.43	0.02

Table 3: Mean conditions during sediment incubations (n = 3)

Parameter	Oxic 6°C	Oxic 20°C	Anoxic 6°C	Anoxic 20°C
pH	8.2 ± 0.3	8.2 ± 0.3	8.5 ±0.01	7.5 ± 0.2
ORP (mV)	461 ± 44	406 ± 23	392 ± 26	-58 ± 79
O_2 [%]	98.1 ± 5.6	95 ± 3.5	2.4 ± 1	<0.005
NO_3-N [mg L^{-1}]	0.22 ± 0.11	0.33 ± 0.20	0.05 ± 0.01	<0.042

802 **Table 4: Benthic fluxes under different temperature and oxygen conditions. Positive**
803 **flux indicates solute release from sediment while negative flux indicates solute loss**
804 **from water. Asterisks denote fluxes not significantly different from zero.**

Parameter [mmol m^{-2} d^{-1}]	**Oxic 6°C**	**Oxic 20°C**	**Anoxic 6°C**	**Anoxic 20°C**
SRP	-0.024 ± 0.02	-0.08 ± 0.03*	0.17±0.06*	0.94 ± 0.23
DP	-0.02 ± 0.03*	0.09 ± 0.05*	0.17 ± 0.07*	0.98 ± 0.21
TP	-0.62 ± 0.64*	0.10 ±0.07*	0.20 ± 0.08*	0.99 ± 0.15
NH_4^+-N	-0.18 ± 0.04	-0.22 ± 0.13*	1.15 ± 0.16	4.86 ± 1.74
NO_3^--N	0.20 ± 0.09*	0.35 ± 0.17*	-0.058 ± 0.003	-0.106 ± 0.008
DOC	-0.97 ± 0.22	-0.70 ± 0.42*	-0.43 ± 0.36*	1.17 ± 0.26
Fe	-0.00006 ± 0.00005*	0.00011 ± 0.00025*	0.00034 ± 0.00039*	0.0019 ± 0.0063*
Mn	-0.026 ± 0.009	-0.080 ± 0.067*	0.79 ± 0.55*	0.66 ± 0.26
SO_4^{2-}	4.60 ± 1.40	3.91 ± 4.41*	-1.68 ± 1.20*	-10.16 ± 2.95
O_2	-25.50 ± 0.10	-43.50 ± 4.60	NA	NA

805